MolecularMedicine

Aloperine Protects Mice against Ischemia-Reperfusion (IR)-Induced Renal Injury by Regulating PI3K/AKT/mTOR Signaling and AP-1 Activity

Shuang Hu,[1] Yuxing Zhang,[1*] Meng Zhang,[1] Yanchao Guo,[1] Ping Yang,[1] Shu Zhang,[1] Sakine Simsekyilmaz,[1] Jun-Fa Xu,[2] Jinxiu Li,[3] Xudong Xiang,[3] Qilin Yu,[1] and Cong-Yi Wang[1,2,3]*

[1]The Center for Biomedical Research, Tongji Hospital, Tongji Medical College, Huazhong University of Science and Technology, Wuhan, China; [2]Department of Clinical Immunology, Institute of Laboratory Medicine, Guangdong Medical College, Dongguan, China; and [3]Department of Emergency Medicine, Institute of Emergency Medicine and Rare Diseases, the Second Xiangya Hospital, Central South University, Changsha, China

Aloperine is a quinolizidine alkaloid extracted from the leaves of Sophora plants. It has been recognized with the potential to treat inflammatory and allergic diseases as well as tumors. In this report, we demonstrate that pretreatment with aloperine provided protection for mice against ischemia-reperfusion (IR)-induced acute renal injury as manifested by the attenuated inflammatory infiltration, reduced tubular apoptosis, and well-preserved renal function. Mechanistic studies revealed that aloperine selectively repressed IL-1β and IFN-γ expression by regulating PI3K/Akt/mTOR signaling and NF-κB transcriptional activity. However, aloperine did not show a perceptible impact on IL-6 and TGF-β expression and the related Jak2/Stat3 signaling. It was also noted that aloperine regulates AP-1 activity, through which it not only enhances SOD expression to increase reactive oxygen species (ROS) detoxification but also promotes the expression of antiapoptotic Bcl-2, thereby preventing tubular cells from IR-induced apoptosis. Collectively, our data suggest that administration of aloperine prior to IR insults, such as renal transplantation, could be a viable approach to prevent IR-induced injuries.

Online address: http://www.molmed.org
doi: 10.2119/molmed.2015.00056

INTRODUCTION

Renal ischemia and reperfusion (IR) injury is one of the major causes of acute kidney disease, a disorder with high morbidity and mortality in clinical settings (1). Indeed, IR inevitably resulted from the consequences of renal transplantation, aortic bypass surgery, and vascular surgery (2–6). There is overwhelming evidence that IR breaks the immune homeostasis by causing changes in endothelial cells, tubular epithelial cells, leukocytes, and renal parenchymal cells (7–11). Particularly, interplay between inflammatory cytokines/chemokines, apoptotic factors and reactive oxygen species (ROS) has been observed during the course of IR-induced renal injury (12–15). Because of this complexity, its underlying molecular mechanisms remained poorly understood (16,17). It is believed that the innate immune system is activated in the very early stage of IR insult as manifested by the accumulation of neutrophils, dendritic cells (DCs) and macrophages, followed by the release of copious amounts of inflammatory mediators (18,19). Given that tubular cells are very susceptible to ROS (20–22), renal tubular apoptosis is a characteristic feature for the progression of IR insult (23).

Previous studies have consistently demonstrated that aloperine, an alkaloid extracted from *sophora alopecuroides*, possesses beneficial properties against inflammation, tumor growth and infection (24–28). As a result, it has been used widely in clinical settings for the treatment of inflammatory diseases including allergic dermatitis (29). More interestingly, recent studies further suggest the potential for aloperine to attenuate oxidative stress (30). These findings prompted us to hypothesize that aloperine could be a good candidate drug for the prevention and treatment of IR-induced acute renal injury. To address this feasibility, we conducted studies in mice

*SH and YZ contributed equally to this work.

Address correspondence to *Cong-Yi Wang and Qilin Yu, The Center for Biomedical Research, Tongji Hospital, Huazhong University of Science and Technology, 1095 Jiefang Avenue, Wuhan, 430030, China. Phone: +86-27-8366-3485; Fax: +86-27-8366-3486. E-mail: wangcy@tjh.tjmu.edu.cn or lyu@tjh.tjmu.edu.cn.*

Submitted April 16, 2015; Accepted for publication October 27, 2015; Published Online (www.molmed.org) November 3, 2015.

with IR insult. Our results revealed that pretreatment with aloperine provided protection for mice against IR-induced acute renal injury as manifested by the attenuated inflammatory infiltration and reduced tubular apoptosis along with improved renal function. Our data suggest that administration of aloperine prior to IR insults could be a viable approach to the prevention of IR-induced renal injuries in clinical settings.

MATERIALS AND METHODS

Animals

Male *C57BL/six mice* (7 wks old, bodyweight 25-30 g) were purchased from the Animal Experimental Center of Hubei Province (Wuhan, China) and housed in a specific pathogen-free facility with free access to sterile acidified water and irradiated food. After a minimum acclimation of 1 wk, the mice were randomly allocated into four groups, each containing six mice: i) IR-aloperine group (IR + Alo) mice were pretreated with 50 mg/kg bodyweight of aloperine (Q1962, Kmaels) dissolved in saline containing 10% acetic acid (2.5 mg/mL), by gavage for 8 consecutive days before IR insult; ii) I/R-vehicle group (IR) mice were pretreated with 10% acetic acid in normal saline as above followed by IR insult; iii) Sham group (Sham) mice underwent similar surgical procedures but without IR insult; and iv) Sham-aloperine group (Sham + Alo) mice were administered with the same dose of aloperine as above. The aloperine dose (50 mg/kg) was optimized by pilot experiments, and no cytotoxicity was observed until the dosage reached 150 mg/kg for 8 consecutive days. All studies were conducted according to the NIH guidelines (*Guide for the Care and Use of Laboratory Animals*, 8th edition, 2011) and approved by the Institutional Animal Care and Use Committee at the Tongji Hospital, Huazhong University of Science and Technology.

Cell Culture

RAW264.7 and HK2 cells were cultured in the complete RPMI-1640 medium containing 10% FBS and 1% antibiotics (100 IU/mL penicillin, 100 μg/mL streptomycin) at 37°C under 5% CO_2 for 24 h, then subjected to serum starvation for 24 h by reducing FBS to 2%. After washes, the monolayer was immersed in mineral oil for 3 h, followed by culturing the cells under normal conditions for another 24 h as reported (31,32). HK2 and RAW264.7 cultures were divided into four groups: i) normal control (Nor) cells were cultured under normal condition; ii) hypoxic control (Hypo) cells were subjected to hypoxic insult; iii) hypoxia + aloperine (Hypo + Alo) cells underwent hypoxic insult in the presence of 0.5 mmol/L aloperine; and iv) hypoxia + aloperine + Tanshinone IIA (an inhibitor of for AP-1) (Hypo + Alo + TanIIA) cells were subjected to hypoxia in the presence of aloperine and Tanshinone IIA (TanIIA, 8 μg/mL).

Induction of Renal IR Injury

The mice were anesthetized by intraperitoneal (IP) injection of 1% pentobarbital (80 mg/kg bodyweight), and then placed in a prone position on a heating pad to maintain their body temperature during surgery. After bilateral flank 1-cm incisions, both kidneys were subjected to ischemia for 45 min using microvascular clamps (0.75-mm clip width and 5-mm jaw length, RoBoz Surgical Instrument Co.) and then reperfused as previously described (33). All mice were administered 200 μL of saline through subcutaneous injection to maintain fluid balance. After the surgery, the mice had access to food and water ad libitum. Mice were killed 24 h after reperfusion. Plasma samples and renal tissues were collected for experimental purposes.

Assessment of Renal Function

Renal function was assessed by measuring blood urea nitrogen (BUN) and serum creatinine (Cr) at the Department of Clinical Laboratories of Tongji Hospital.

Histological Analysis

Paraffin embedded renal sections (3 μm) were subjected to hematoxylin and eosin (H&E) and periodic acid-Schiff (PAS) staining as reported previously (34,35). Morphological changes in the cortex and medulla were scored in a blinded fashion by two pathologists according to the severity of tubular necrosis, integrity of brush border and basement membrane, and cast formation. The scoring included 4 scales: 0) <10%; 1) 10% to 25%; 2) 25% to 50%; 3) 50% to 75%; and 4) >75% (36). Each section was assessed with randomly selected 10 high-power fields (magnification, × 400), and three mice were included in each study group.

Myeloperoxidase (MPO) and F4/80 Immunostaining

Renal sections were deparaffinized and treated with proteinase K (Merck). The sections were first treated with 3% H_2O_2 to block endogenous peroxidase activity, followed by incubation with antibodies against F4/80 antibody (ABD) (Serotec Inc.) and MPO (Thermo Scientific), respectively. After washes with PBS, the sections were incubated with a biotinylated anti-rat IgG (ZSJQ-BIO). The sections were then developed using a Vector stain ABC kit (Vector Laboratories Inc.), and further counterstained with Harris hematoxylin as reported previously (37). Assessment of neutrophil and macrophage infiltration was carried out in a blinded fashion under a microscope by counting the MPO- or F4/80-positive cells per field with 10 randomly selected fields per section at magnification of 400×; three mice were examined in each study group.

Real-Time PCR Analysis

Renal total RNA extraction and cDNA synthesis were conducted using the established techniques (38). Real-time PCR was then carried out using an ABI prism 7500 Sequence Detection System (Applied Biosystems) with primers specific for *IL-1β* (5′-GGA TGA GGA CAT GAG CAC CT-3′, 5′-GGA GCC TGT AGT GCA GTT GT-3′), *IL-10* (5′-CCC TTT GCT ATG GTG TCC TT-3′, 5′-TGG TTT CTC TTC CCA AGA CC-3′), *IFN-γ* (5′-GGC ACA GTC ATT GAA AGC CTA-3′, 5′-CTG CAG GAT TTT CAT

GTC ACC-3′), *IL-6* (5′-AGT TGC CTT CTT GGG ACT GA-3′, 5′-TCC ACG ATT TCC CAG AGA AC-3′), and *TGF-β* (5′-CAA CAA TTC CTG GCG TTA CCT TGG-3′, 5′-GAA AGC CCT GTA TTC CGT CTC CTT-3′). Glyceralhyde-3-phosphate dehydrogenase (*GAPDH*) was used for normalization (5′-TGG CAT TGT GGA AGG GCT CA-3′, 5′-GCA CCA GTG GAT GCA GGG AT-3′). PCR amplifications were carried out at 95°C for 1 min, followed by 40 cycles at 95°C for 15 sec, 60°C for 1 min. Relative expression levels for each target gene were calculated using the $2^{-\Delta\Delta Ct}$ approach (38).

Assays for ROS Accumulation, MDA Level and SOD Activity

For analysis of ROS accumulation, fresh frozen sections were incubated with 2′ 7′–dichlorodihydrofluorescein diacetate (DCFH-DA, 10 μmol/L, YIJI) at 37°C for 25 min. After washes, the sections were subjected to fluorescence analysis under a fluorescence microscope (Olympus, Japan). The intensity of fluorescence on each section was analyzed using the Image Pro Plus software (Media Cybernetics) as reported (39). SOD activity and MDA levels were measured by the commercial kits from Nanjing Jiancheng Bioengineering Institute according to their respective instructions.

Western Blot Analysis

Cell or renal lysates (50 μg) were separated on 10% polyacrylamide gel (Sigma-Aldrich) and transferred onto PVDF membranes. The membranes were blocked with 5% nonfat milk for 1 h and then incubated with antibodies with optimal dilutions against PI3Kp85, p-PI3Kp85, AKT, p-AKT, mTOR, p-mTOR, Bcl2, c-Fos, Jak2, p-Jak2, Stat3, p-Stat3 (all Cell Signaling Technology), GAPDH, lamin B, caspase-3 and NF-κBp65 (all Santa Cruz Technologies) overnight at 4°C. After six washes (each for 5 min), the membranes were probed with an HRP-conjugated secondary antibody and then visualized using an ECL Plus Western blot kit (PIERCE) as reported previously (40). GAPDH was used for normalization, and the intensity of each reactive band was analyzed using the densitometry plugin ImageJ software (http://rsb.info.nih.gov/ij/) as instructed.

Terminal Deoxynucleotidyl Transferase dUTP Conjugated with Fluorescein (TUNEL) Assay

Apoptotic cells in renal sections were estimated by TUNEL assay using a kit from Roche Diagnostics using the established techniques (41). Apoptotic rate was assessed by averaging the total number of apoptotic cells in 10 randomly selected fields at 400 × magnification of each section in a blinded manner. Three sections were examined for each mouse and three mice were included in each study group.

Electrophoretic Mobility Shift Assay (EMSA)

Nuclear proteins derived from HK2 cells and macrophages were prepared using the NE-PER Nuclear and Cytoplasmic Extraction Reagents (Thermo Scientific), and then subjected to EMSA using a LightShift Chemiluminescent EMSA Kit (Thermo Scientific) as described previously (34). Biotin-labeled double-stranded oligonucleotides containing the NF-κbp65 (biotin-5′-AGT TGA GGG GAC TTT CCC AGG C-3′, biotin-5′-GCC TGG GAA AGT CCC CTC AAC T-3′) or AP-1 binding site (biotin-5′-CGC TTG ATG ACT CAG CCG GAA-3′, biotin-5′-TTC CGG CTG AGT CAT CAA GCG-3′) (Beyotime) were used as the probe for analysis of NF-κB and AP-1 DNA binding activity, respectively. A mixture of unlabeled probes was used as a negative control.

Statistical Analysis

All data are present as mean ± SEM, and all *in vitro* experiments were conducted with at least three independent replications. A P value of <0.05 was considered statistically significant. The GraphPad Prism 5 software was employed for statistical analysis using Student t test or one-way or two-way ANOVA where appropriate.

All supplementary materials are available online at www.molmed.org.

RESULTS

Aloperine Provides Protection for Mice against IR-Induced Acute Renal Injury

We first sought to assess the effect of aloperine pretreatment on IR-induced acute renal injury. For this purpose, the mice were administered with aloperine for 8 consecutive days, followed by IR insult (IR + Alo group) as described. Mice pretreated with vehicle (IR group) or that had undergone similar surgical processes absent of IR insult (Sham group) or Sham mice pretreated with aloperine (Sham + Alo group) served as controls. Sham + Alo mice manifested similar levels of BUN (Figure 1A) and Cr (Figure 1B) as that of Sham mice, indicating that the administration of aloperine did not result in a perceptible change in renal function. As expected, IR insult led to a significant impairment of renal function. However, aloperine-pretreated mice displayed a well preserved renal function as manifested by the significantly lower levels of serum BUN (Figure 1A) and Cr (Figure 1B) as compared with that of mice from IR group. To confirm these observations, we conducted a histological analysis of renal sections. Indeed, unlike IR + Alo mice, H&E staining revealed that IR mice incurred remarkable tubular injury as evidenced by the severe tubular necrosis, dilation and cast formation (Figure 1C). Similarly, PAS staining demonstrated higher severity for loss of brush border and disintegrity of basement membrane in IR mice compared with that of IR + Alo mice (Figure 1D). Together, our data support that administration of aloperine provides protection for mice against IR-induced acute renal injury.

Aloperine Pretreatment Attenuates IR-Induced Inflammatory Response

To demonstrate whether the alleviated IR injury in mice from IR + Alo group was due to attenuated inflammatory response, we first examined interstitial

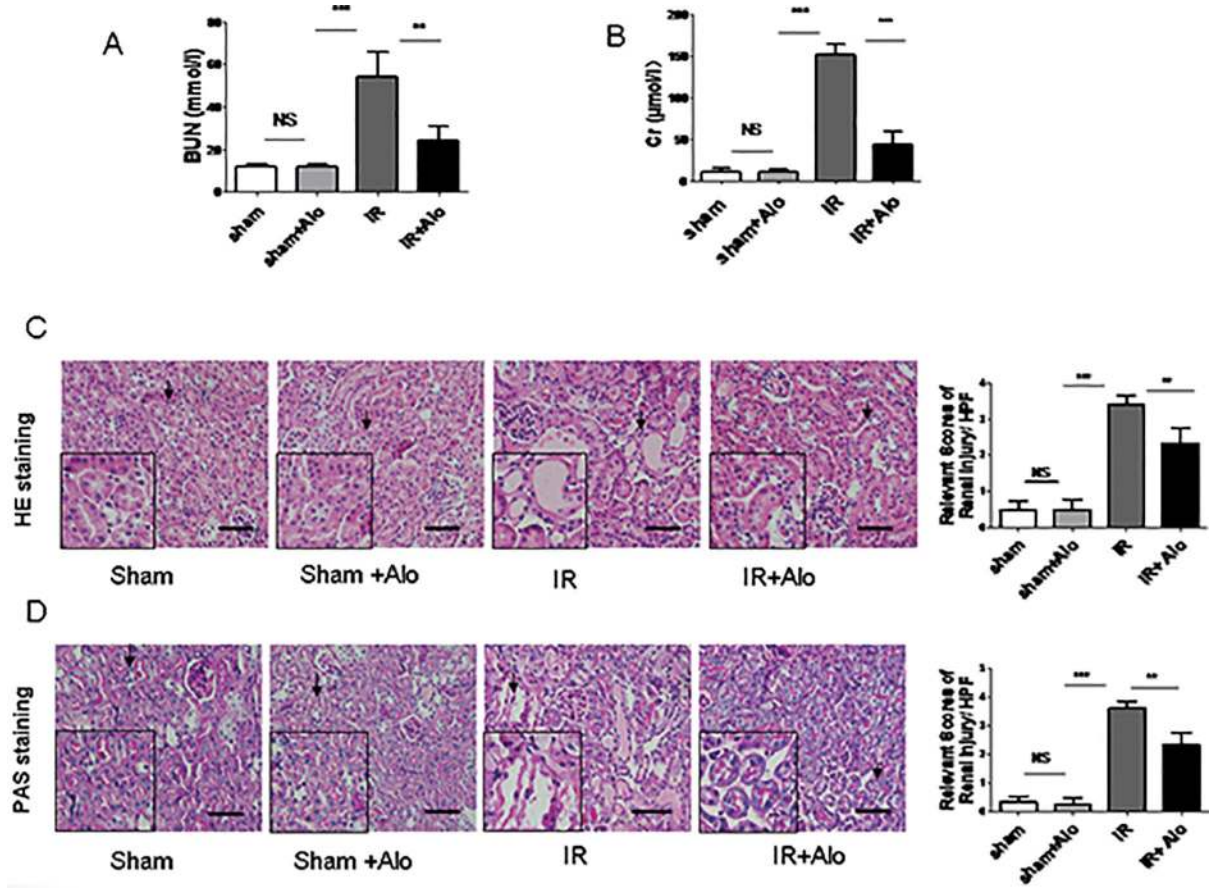

Figure 1. Pretreatment of mice with aloperine attenuates IR-induced renal injury. Sham-operated mice were served as a negative control. (A) Serum creatinine (Cr) levels. (B) Levels for blood urea nitrogen (BUN). Aloperine-pretreated mice manifested significantly lower Cr and BUN as compared with that of mice from the IR group. (C) Results for HE staining of renal sections. The severity of renal injury was assessed as semiquantitative scores based on inflammatory infiltration and tubular necrosis. (D) Results for PAS staining of renal sections. Similarly, the severity of renal injury was assessed as semiquantitative scores based on the integrity of brush border and basement membrane. Cast formation was assessed as mean ± SEM of six mice analyzed for each group. Scale bar = 100 μm. *, $P < 0.05$; **, $P < 0.01$; and ***, $P < 0.001$.

infiltration of neutrophils (MPO^+ cells) and macrophages ($F4/80^+$ cells) in renal sections, respectively. As expected, MPO^+ neutrophils (Figure 2A) and $F4/80^+$ macrophages (Figure 2B) were almost absent in Sham mice and Sham + Alo mice. However, a significant inflammatory infiltration was detected in IR mice, while pretreatment of mice with aloperine (IR + Alo group) significantly attenuated IR-induced inflammatory infiltration as evidenced by the reduction of infiltrated neutrophils (Figure 2A) and macrophages (Figure 2B).

To confirm the above observations, we then assessed inflammatory cytokine production in the kidneys, in which we initially analyzed inflammatory cytokines IL-1β and IFN-γ and antiinflammatory cytokine IL-10 by real-time PCR. Because no discernable difference was noted between Sham mice and Sham + Alo mice in terms of renal function and inflammatory infiltration, we employed only Sham mice as controls for the following studies. In general, only low levels of IL-1β, IFN-γ and IL-10 were detected in Sham mice. However, IR insult induced a significant upregulation for IL-1β (Figure 3A) and IFN-γ (Figure 3B), but no perceptible change was noted for IL-10 (Figure 3C). In sharp contrast, administration of aloperine significantly attenuated IR-induced IL-1β (Figure 3A) and IFN-γ expression (Figure 3B), but a four-fold increase for IL-10 expression was noted in these mice (Figure 3C). These results prompted us to examine additional inflammatory cytokine IL-6 and antiinflammatory cytokine TGF-β. Interestingly, IL-6 was almost absent in Sham mice, while IR insult induced high levels of IL-6 expression in mice from both IR and IR + Alo groups, and particularly, no perceptible effect was noted for aloperine pretreatment in terms of IR-induced IL-6 expression (Figure 3D). Similarly, IR insult induced high levels of TGF-β expression, but no significant difference was noted between mice originated from the IR and IR + Alo groups (Figure 3E). Taken together,

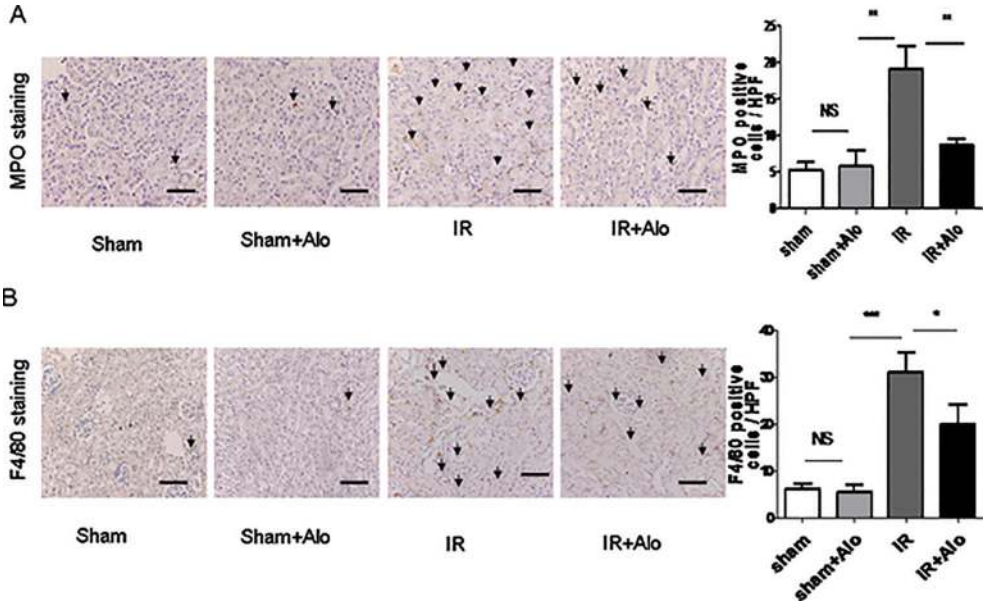

Figure 2. Analysis of inflammatory infiltration of renal sections. Renal sections were prepared 24 h after IR insult. (A) Results for analysis of neutrophil infiltration. Left panel: Representative results for MPO staining. Right panel: Results for quantitative analysis of neutrophil infiltration as mean ± SEM of six mice analyzed for each group. (B) Results for analysis of macrophages infiltration. Left panel: Representative results for F4/80 staining. Right panel: Results for quantitative analysis of macrophage infiltration as mean ± SEM of six mice analyzed for each group. Scale bar = 100 μm. *, $P < 0.05$; **, $P < 0.01$; and ***, $P < 0.001$.

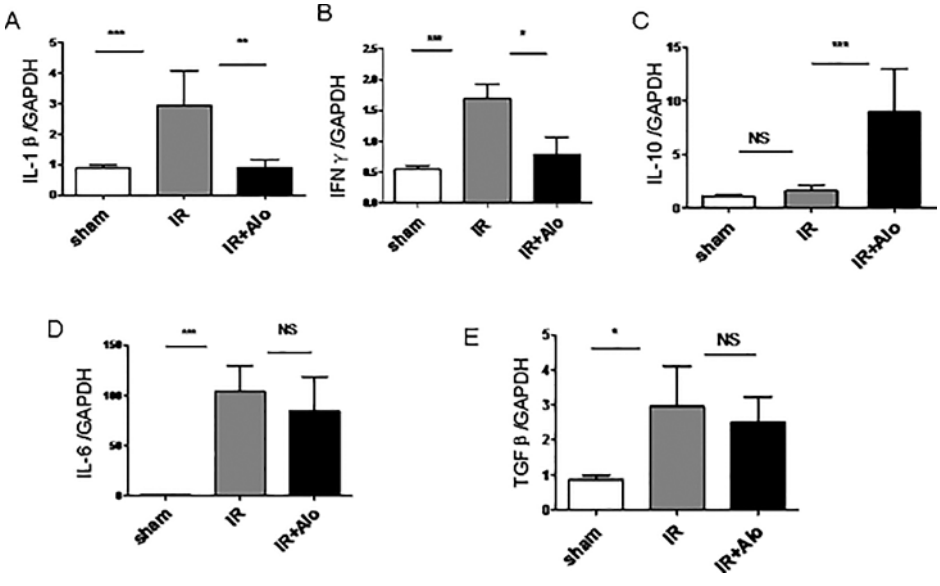

Figure 3. Aloperine pretreatment represses inflammatory cytokine production in the kidneys. Real-time PCR was employed to assess the production of inflammatory cytokines. Pretreatment of mice with aloperine significantly repressed IR-induced (A) IL-1β and (B) IFN-γ expression, but enhanced the expression of (C) antiinflammatory cytokine IL-10. Nevertheless, aloperine pretreatment failed to show a significant impact on (D) IL-6 and (E) TGF-β expression although IR insult induced a significant increase for both cytokines. Panels (A–E) present quantitative analysis as mean ± SEM of six mice analyzed for each group. NS: not significant; *, $P < 0.05$; **, $P < 0.01$; and ***, $P < 0.001$.

these results suggest that aloperine pretreatment specifically attenuates IR-induced IL-1β and IFN-γ production, but potently enhances IL-10 secretion to limit inflammatory response following IR insult.

Administration of Aloperine Prevents IR-Induced Tubular Apoptosis

Because tubular apoptosis is a crucial event in IR-induced renal injury and drives the severity of tissue damage (42,43), we next examined the impact of aloperine pretreatment on IR-induced tubular apoptosis by TUNEL assay. TUNEL-positive cells were almost absent in the sections of mice from Sham group, while a substantial increase of apoptotic cells was noted in IR mice (Figure 4A). However, IR + Alo mice manifested a two-fold reduction of apoptotic cells as compared with that IR mice (Figure 4B), indicating that aloperine pretreatment prevented IR-induced tubular apoptosis. To confirm this conclusion, we further examined caspase 3 levels by Western

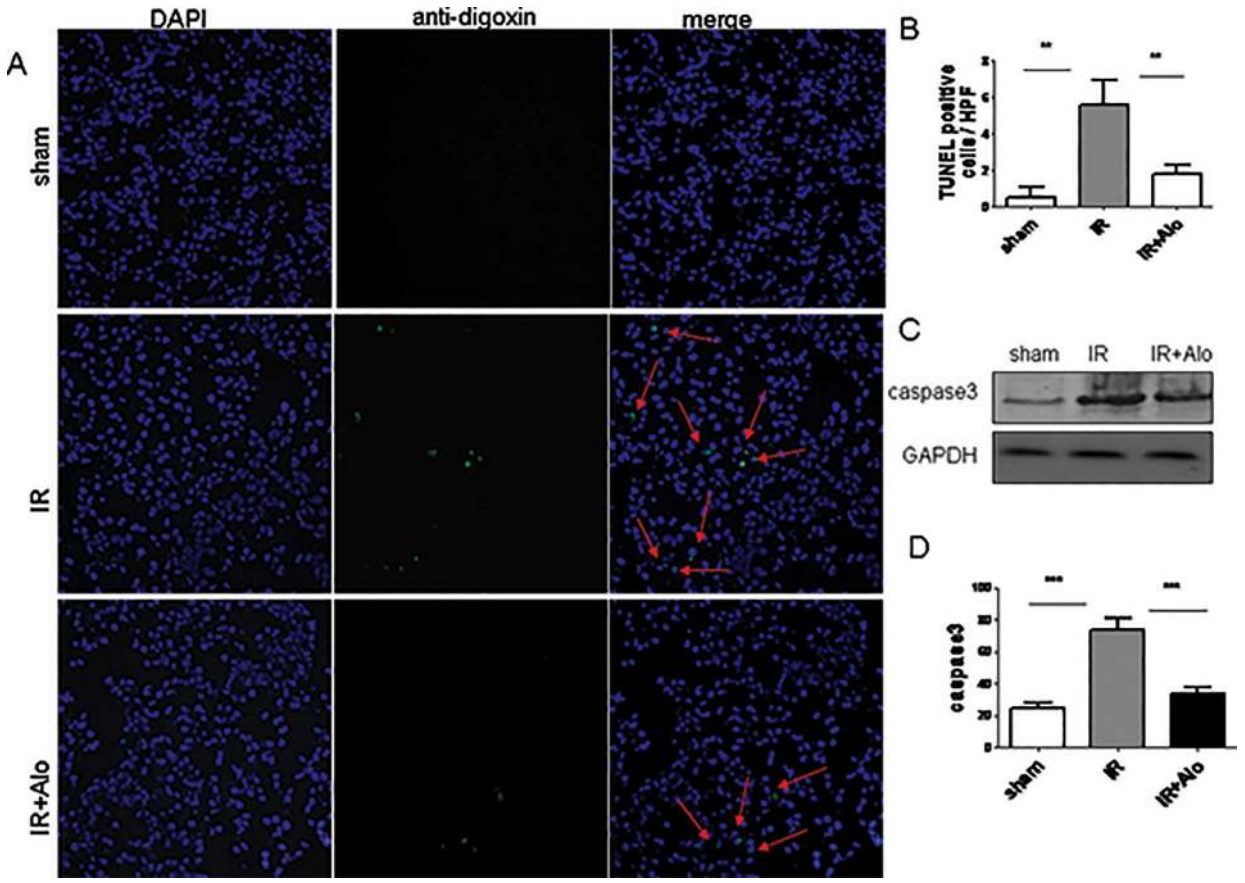

Figure 4. TUNEL assay for analysis of tubular apoptosis. TUNEL assay and Western blot analysis of caspase 3 levels were employed for the assessment of tubular apoptosis. (A) Representative results for TUNEL assays of renal sections (magnification 400×). (B) Quantitative analysis of TUNEL positive cells as mean ± SEM of six mice analyzed for each group. (C) Representative results for Western blot analysis of caspase 3 levels in the kidneys. (D) Relative expression levels for caspase 3 by densitometric analysis as mean ± SEM of six mice analyzed for each group. **, $P < 0.01$; and ***, $P < 0.001$.

blot analysis (Figure 4C). Indeed, aloperine pretreatment resulted in a 1.3-fold reduction for caspase 3 as compared with that of IR mice (Figure 4D).

Aloperine Pretreatment Reduces IR-Induced ROS Accumulation

Given that oxidative stress caused by ROS accumulation plays a critical role in IR-induced tubular apoptosis (44), we investigated ROS accumulation in renal sections by staining with DCFH-DA. It was interestingly noted that IR mice manifested a significant ROS accumulation as compared with that of Sham mice, while aloperine pretreatment led to a 70% reduction of ROS accumulation (Figure 5A). To dissect the mechanism underlying aloperine attenuation of ROS accumulation, we examined the activity of superoxide dismutase (SOD), a critical enzyme responsible for the detoxification of ROS. Surprisingly, IR insult resulted in a significant reduction of SOD activity, while no discernable change in terms of SOD activity was noted between mice from the Sham and IR + Alo groups (Figure 5B), suggesting that aloperine represses ROS accumulation by enhancing SOD activity. We then examined the content of lipid peroxidation end product, malondialdehyde (MDA), in the renal lysates, but no perceptible change was noted (Figure 5C), suggesting that lipid peroxidation is probably not involved in IR-induced renal injury in our model.

Aloperine Suppresses PI3K/Akt/mTOR Signaling and NF-κB Activity

To gain insight into the mechanisms underlying aloperine inhibition of IL-1β and IFN-γ expression, we first examined the activities of MAP kinases ERK1/2 (Supplementary Figure 1A), p38 (Supplementary Figure 1B) and JNK (Supplementary Figure 1C) by Western blot analysis. Unexpectedly, no differences were detected in terms of total and phosphorylated forms between all experimental groups 24 h after IR insult, and similar results were obtained at earlier time points such as 6 and 12 h after IR insult (data not shown). These results prompted us to examine the PI3K/Akt/mTOR signaling. Interestingly, IR insult

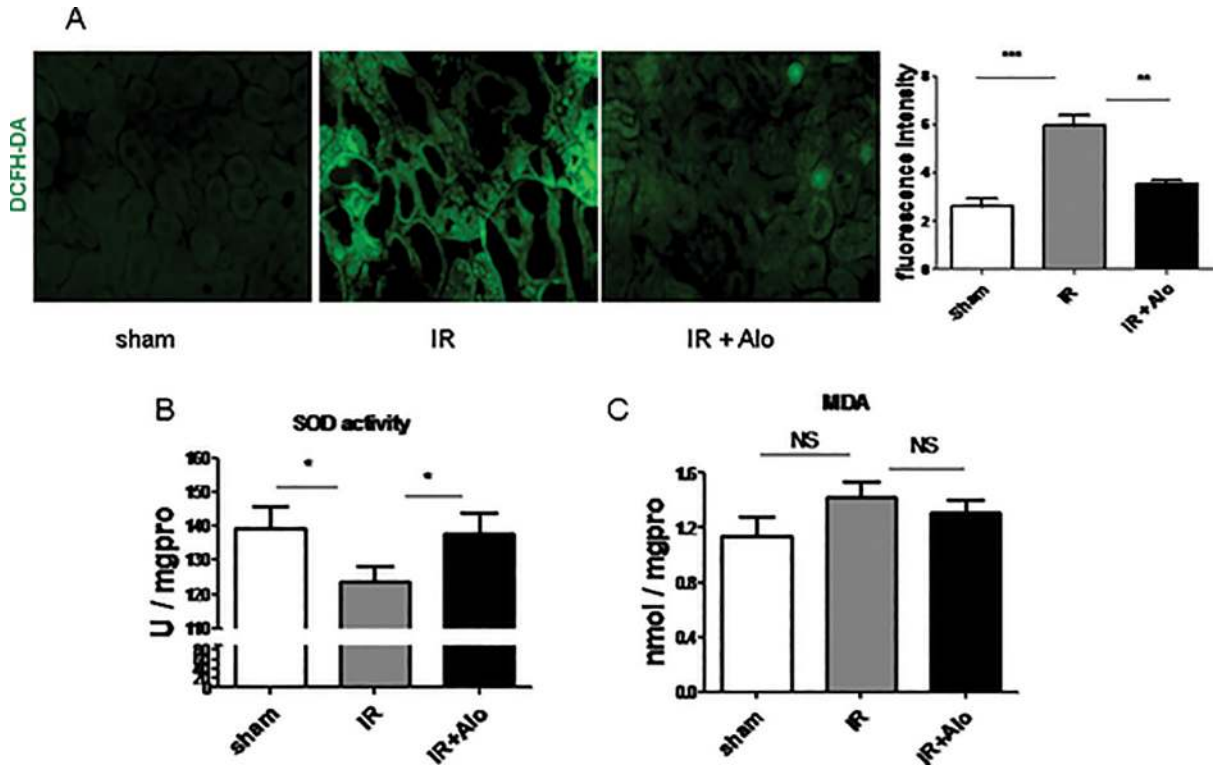

Figure 5. Analysis of oxidative stress in the kidneys after IR insult. (A) Analysis of ROS accumulation. Left panel: representative images for the detection of DCFH-DA fluorescence in the renal sections. Right panel: quantitative analysis of fluorescence intensity of all mice examined. (B) Analysis of SOD activity in the kidneys. IR insult led to a significant reduction of SOD activity, while aloperine pretreatment almost completely restored SOD activity. (C) Analysis of MDA levels in renal lysates. Panels (A–C) present quantitative analysis as mean ± SEM of six mice analyzed for each group. *, $P < 0.05$; **, $P < 0.01$; and ***, $P < 0.001$.

significantly induced PI3K activation as manifested by the increase of p-PI3Kp85 levels, while aloperine pretreatment significantly attenuated IR-induced PI3K activation (Figure 6A). In line with this result, significantly lower activities for its downstream molecules Akt (Figure 6B) and mTOR (Figure 6C) were noted in aloperine-pretreated mice as compared with that of IR mice. Given that NF-κB is downstream of PI3K/AkT/mTOR signaling, we further investigated NF-κB activation by analysis of phosphorylated p65 (p-p65) in the nucleus. As expected, administration of aloperine significantly inhibited NF-κB activation as evidenced by the significantly reduced p-p65 levels (Figure 6D).

To confirm the above results, we cultured RAW264.7 cells, a murine macrophage cell line, under hypoxic conditions in the presence or absence of aloperine as described, followed by analysis of NF-κB activity. We first conducted Western blot analysis to confirm the effect of aloperine on PI3K/Akt signaling in RAW264.7 cells. Indeed, aloperine significantly attenuated hypoxia-induced PI3Kp85 and Akt activation (Supplementary Figure 1D). Similarly, treatment of RAW264.7 cells with aloperine markedly inhibited hypoxia-induced NF-κB activation as evidenced by the reduced amount of p-p65 in the nucleus (Figure 6E). To further confirm these data, EMSA was employed to assess NF-κB DNA binding activity. It was noted that the addition of aloperine attenuated hypoxia-induced NF-κB DNA binding activity by almost one-fold (Figure 6F). Collectively, our data support that aloperine inhibits PI3K/AkT/mTOR signaling, thereby repressing NF-κB activity to attenuate IL-1β and IFN-γ expression.

Aloperine Enhances AP-1 Activity to Repress Tubular Apoptosis and to Promote IL-10 Secretion

To explore the mechanism by which aloperine enhances SOD activity to prevent ROS accumulation, we examined AP-1 transcriptional activity, a crucial transcription factor responsible for SOD expression. Notably, significantly higher levels of c-Fos were detected in mice pretreated with aloperine as compared with that in IR and Sham mice (Figure 7A), suggesting that aloperine promotes AP-1 activity and thereby enhances SOD expression. Because AP-1 also transcribes the expression of Bcl-2, a critical antiapoptotic molecule (45), we next examined Bcl-2 levels in renal lysates. Consistent with enhanced AP-1 activity, much higher levels of Bcl-2 were detected in aloperine-pretreated mice as compared with PBS-treated mice (IR group) (Figure 7B).

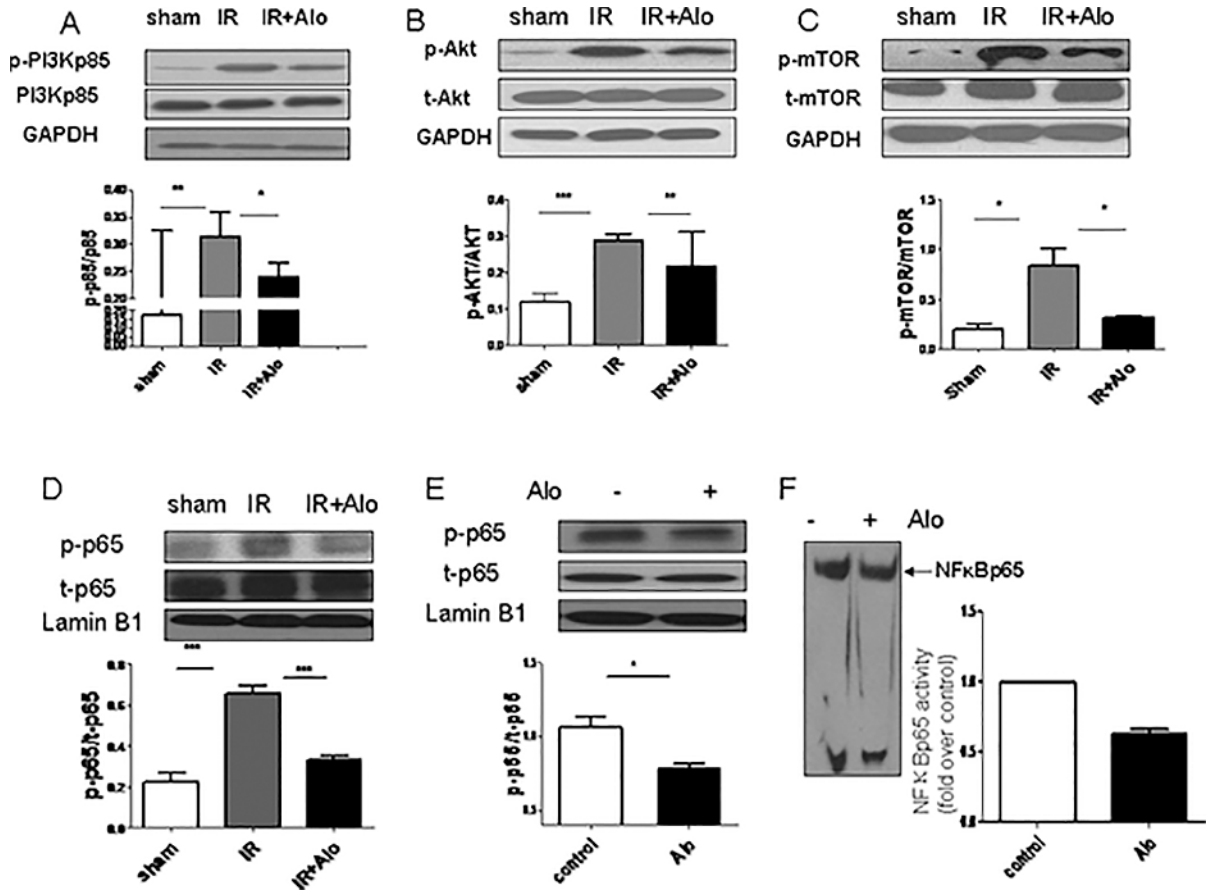

Figure 6. Aloperine regulates PI3K/Akt/mTOR signaling and NF-κB transcriptional activity. (A) Results for analysis of total and phosphorylated PI3Kp85 subunit in renal lysates. (B) Total and phosphorylated Akt in renal lysates. (C) Analysis of total and phosphorylated mTOR in renal lysates. (D) Western blot analysis of nuclear NF-κBp65 activity in the kidneys. (E) Analysis of NF-κBp65 activity in RAW264.7 cells that had undergone hypoxic insult in the presence of aloperine. (F) EMSA results for analysis of NF-κB DNA binding activity in RAW264.7 cells that had undergone hypoxic insult in the presence of aloperine. Panels (A–D) present quantitative analysis as mean ± SEM of six mice analyzed for each group. *, $P < 0.05$; **, $P < 0.01$; and ***, $P < 0.001$.

Next, we cultured HK2 cells, a tubular cell line, under hypoxic conditions as above in the presence of aloperine along with the administration of Tanshinone IIA (TanIIA), an AP-1-inhibitor. Indeed, hypoxia induced a significant upregulation for nuclear c-Fos (Figure 7C) along with enhanced Bcl-2 expression (Figure 7D) as compared with that of cells cultured under normoxic condition. Importantly, significantly higher levels of c-Fos (Figure 7C) and Bcl-2 expression (Figure 7D) were noted in cells cultured with aloperine as compared with cells without aloperine, while the addition of TanIIA almost completely abolished the effect of aloperine. In line with these results, significantly higher AP-1 DNA binding activity was detected in aloperine-treated HK2 cells, which was abrogated by the addition of TanIIA (Figure 7E).

Because AP-1 also serves as a potent transcription factor for IL-10 expression (46), we then treated RAW264.7 cells with aloperine as above in the presence of TanIIA. As expected, aloperine stimulated RAW264.7 cells expression of high levels of IL-10, while blockade of AP-1 activity by TanIIA almost completely abolished aloperine-induced IL-10 expression (Figure 7F), indicating that aloperine enhances IL-10 expression by regulating AP-1 activity. The next important question is why administration of aloperine did not affect IL-6 and TGF-β expression. Given the role that Jak2/Stat3 signaling played in the regulation of IL-6 and TGF-β transcription (47), we conducted Western blot analysis to check the impact of aloperine on Jak2/Stat3 activity. As expected, IR insult induced a significant increase for total Jak2 and phosphorylated Jak2 (p-Jak2) (Figure 7G), and also for total Stat3 and phosphorylated Stat3 (p-Stat3) (Figure 7H). However, we failed to detect a perceptible difference between IR and IR + Alo mice. To confirm this observation, we further examined Jak2/Stat3 signaling in the above-prepared RAW264.7 and HK2 cells with hypoxic insult, and similar results were obtained

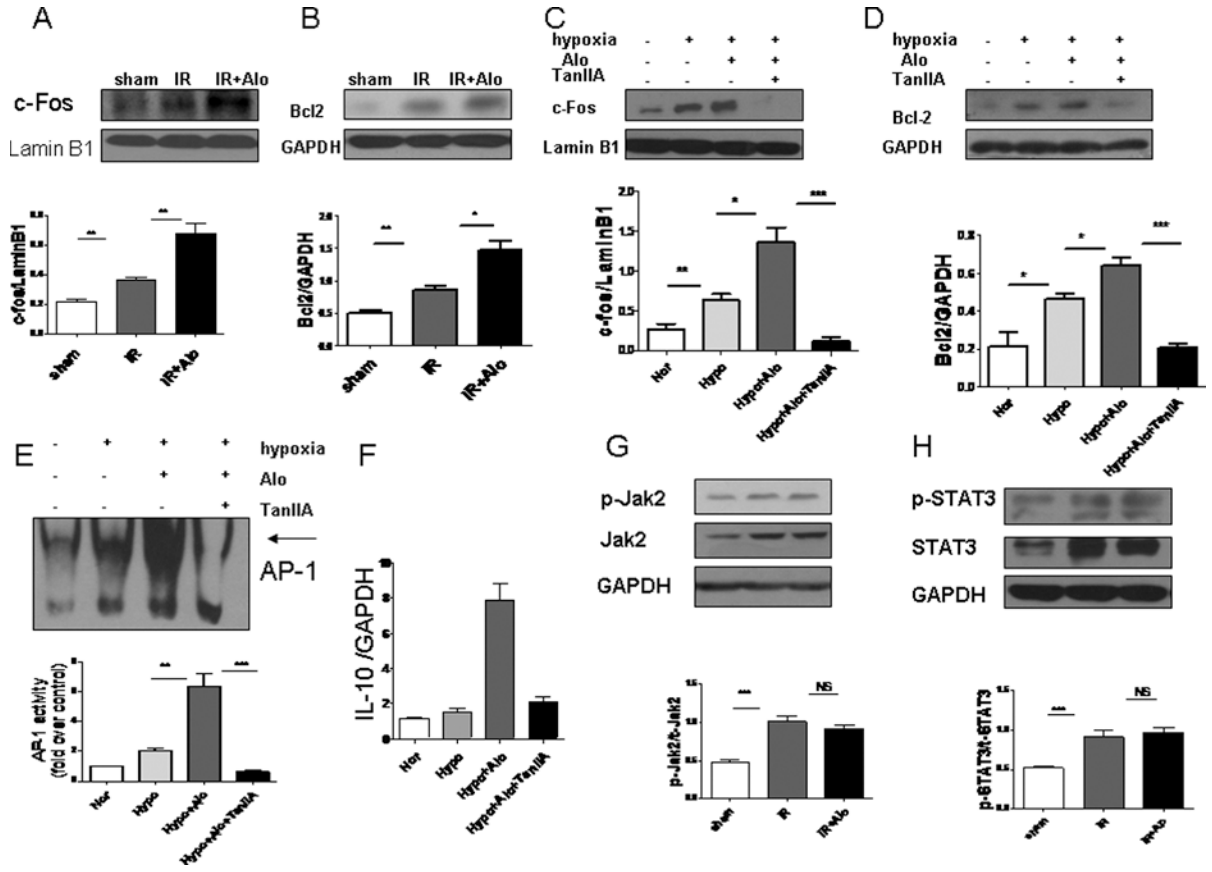

Figure 7. The impact of aloperine pretreatment on AP-1 activity. (A) Analysis of nuclear AP-1 subunit c-Fos expression in renal lysates. (B) Western blot results for analysis of Bcl-2 in renal lysates. (C) Analysis of nuclear c-Fos levels in HK2 cells that had undergone hypoxic insult in the presence of aloperine along with administration of TanIIA. (D) Western blot analysis of Bcl-2 expression in the above prepared HK2 cells. (E) EMSA results for analysis of AP-1 DNA-binding activity in the above prepared HK2 cells. (F) TanIIA abrogated aloperine-induced IL-10 expression in RAW264.7 cells following hypoxic insult. (G) Western blot analysis for total and phosphorylated Jak2 levels in renal lysates of mice that had undergone IR insult. (H) Total and phosphorylated Stat3 in the kidneys of mice after IR insult. Panels (A, B, G, H) present quantitative analysis as mean ± SEM of six mice analyzed for each group.*, $P < 0.05$; **, $P < 0.01$; and ***, $P < 0.001$.

(data not shown). Collectively, these data suggest that aloperine selectively regulates PI3K/Akt signaling and AP-1 activity, but does not affect Jak2/Stat3 signaling and, as a result, administration of aloperine did not result in a significant change for IL-6 and TGF-β expression.

DISCUSSION

Although aloperine has been recognized with therapeutic potential for inflammatory and allergic diseases in clinical settings (28,29), its effect on IR-induced acute renal injury, however, has yet to be elucidated. In this study, we induced mice with 45 min ischemia along with aloperine precondition followed by reperfusion, and IR injury was assessed 24 h after reperfusion. We demonstrated convincing evidence suggesting that pretreatment with aloperine provides protection for mice against IR-induced acute renal injury as manifested by the well preserved renal function along with attenuated pathological changes and inflammatory infiltration. Our data support that aloperine could be an alternative therapy for prevention of IR injury in clinical settings.

IL-1β, one of the most important proinflammatory cytokines, is generally produced at sites of tissue injury or infection by infiltrated immune cells (48). Similarly, IFN-γ is another potent proinflammatory cytokine playing a central role in inflammatory responses (49). By contrast, IL-10 possesses antiinflammatory properties in limiting host immune response to pathogens or tissue injury (50). Consistent with the role both IL-1β and IFN-γ played during the course of inflammatory responses, IR insult resulted in a significant upregulation of IL-1β and IFN-γ in the kidneys. However, pretreatment of mice with aloperine markedly attenuated renal IL-1β and IFN-γ expression, but the expression of IL-10 was increased by four-fold, indicating that aloperine protects mice against IR-induced injury by repressing inflammatory responses. Interestingly, unlike its effect on

IL-1β and IFN-γ, we failed to obtain data supporting that aloperine modulates IL-6 and TGF-β expression.

The mechanisms underlying IR-induced acute renal injury are complex and have yet to be fully elucidated. However, MAP kinases and PI3K/Akt/mTOR signaling are thought to be implicated in the initiation and progression of IR-induced inflammatory responses (51–54). We first examined the impact of aloperine on MAP kinase activities. Unexpectedly, we failed to detect a perceptible change in terms of the expression for total and activated (phosphorylated) ERK1/2, p38 and JNK, suggesting that MAP kinases are not relevant to an aloperine-mediated protective effect in our model. These results prompted us to embark on the PI3K/Akt/mTOR signaling, which is well known to regulate a variety of essential cellular functions ranging from glucose metabolism, protein synthesis, cell proliferation, apoptosis and survival (55–58). PI3K consists of two elements, the regulatory subunit p85 and the catalytic subunit p110 (22,59). Its function relies on the activation of p85. Unlike its effect on MAP kinases, mice pretreated with aloperine manifested significantly attenuated levels for phosphorylated PI3Kp85, Akt and mTOR, while total PI3Kp85, Akt and mTOR were not changed. In line with these results, the phosphorylated levels for NF-κBp65 in the nucleus were reduced significantly in aloperine-pretreated mice as compared with that of IR mice. Indeed, RAW264.7 cells cultured under hypoxic conditions in the presence of aloperine manifested attenuated PI3K/Akt/mTOR signaling, which then repressed the activation of NF-κBp65 along with reduced DNA activity. In looking at this data together, our results suggest that aloperine attenuates inflammatory responses in the setting of IR-induced acute renal injury by repressing PI3K/Akt/mTOR signaling and NF-κB transcriptional activity. In support of this conclusion, PI3K/Akt/mTOR signaling has already been recognized to play a crucial role in inflammatory infiltration (60,61) and IR-induced cardiac injury (62,63). However, we cannot exclude the feasibility that aloperine regulates additional pathways other than the PI3K/Akt/mTOR signaling in the setting of IR-induced acute renal injury. In addition, the detailed mechanisms underlying aloperine repression of PI3K signaling remain to be elucidated and would be a major focus for future studies. It is worth noting that aloperine did not regulate Jak2/Stat3 signaling, a critical pathway for IL-6 and TGF-β transcription, and, therefore, IL-6 and TGF-β expression were not affected following aloperine treatment. However, previous studies also suggested that the transcription of IL-6 can be regulated by NF-κB as well (64). The confliction between our current report and previous studies could be caused by the differences in experimental system and cell types. Also, our data could be a consequence of interplay between NF-κB and Jak2/Stat3 signaling.

Programmed death of tubular cells is another critical characteristic feature relevant to IR-induced acute renal injury (65). Indeed, IR insult rendered tubular cells undergoing apoptosis along with upregulation of caspase-3. However, pretreatment of mice with aloperine prevented tubular cells from IR-induced apoptosis as evidenced by the significant reduction of TUNEL-positive tubular cells and decreased protein levels for caspase-3. This finding somehow is in conflict with studies in tumor cells in which aloperine was noted to promote cancer or tumor cell apoptosis (26,66). To confirm this observation, we cultured HK2 cells under hypoxic conditions in the presence of aloperine and similar results were obtained (data not shown). In the setting of cancer therapy, high doses of aloperine were employed to generate cytotoxicity for killing tumor cells, and therefore, it is likely that this discrepancy was caused by the differences of aloperine doses.

Given that oxidative stress caused by a burst of ROS generation and a decrease of antioxidants is a critical feature in IR-induced tubular apoptosis (44), we next examined the impact of aloperine on IR-induced ROS accumulation. As expected, IR insult induced a significant accumulation of ROS in the kidneys. However, pretreatment of mice with aloperine significantly prevented ROS accumulation as manifested by the reduction of fluorescence intensity. We then checked SOD activity, a critical enzyme responsible for the detoxification of ROS. It was noted that mice that had undergone IR insult manifested a significant reduction of SOD activity, while pretreatment of mice with aloperine almost completely prevented IR-induced suppression of SOD activity, suggesting that IR-induced ROS accumulation is at least in part caused by the impaired capability for ROS detoxification. Nevertheless, lipid peroxidation is unlikely involved in the induction of oxidative stress in our model as no difference was noted for MDA between all groups of mice. Of important note, in contrast to our observations in IR-induced acute renal injury, a previous study suggested that aloperine was able to reduce the content of MDA in hepatic tissue of intoxicated animals without affecting SOD activity (28). This discrepancy might be due to the differences of animal models employed.

To further address the mechanisms relevant to enhanced SOD activity and repressed tubular apoptosis, we checked AP-1 activity as it is a crucial factor responsible for SOD expression and antiapoptotic Bcl-2 transcription (45,67). Excitingly, renal lysates originated from aloperine-pretreated mice displayed a significant increase for nuclear AP-1 subunit c-Fos along with enhanced Bcl-2 expression. To confirm those results, we further examined HK2 lysates that had undergone hypoxic insult. Indeed, the addition of aloperine significantly enhanced hypoxia-induced nuclear c-Fos and antiapoptotic Bcl-2 expression, which was completely abrogated by the addition of TanIIA, an AP-1 inhibitor. Collectively, our data support that aloperine regulates AP-1 activity, by which it enhances SOD expression

to promote ROS detoxification along with an increase of antiapoptotic Bcl-2 expression, thereby protecting tubular cells from IR-induced apoptosis. Interestingly, blockade of AP-1 activity in RAW264.7 cells by the addition of TanIIA almost completely abolished aloperine-induced IL-10 expression, indicating that aloperine promotes IL-10 expression by enhancing AP-1 activity as well. Of important note, PI3K/Akt signaling has been suggested to serve as a survival signal during renal IR (68) and, as a result, aloperine protection of IR-induced tubular apoptosis could be a compromised effect from the homeostasis of multiple signaling pathways.

CONCLUSION

In summary, we demonstrated convincing evidence that pretreatment of mice with aloperine provides protection against IR-induced acute renal injury as manifested by the attenuated inflammatory infiltration, reduced tubular apoptosis along with well preserved renal function. Mechanistic studies revealed that aloperine selectively represses IL-1β and IFN-γ expression by regulating PI3K/Akt/mTOR signaling and NF-κB transcriptional activity. Aloperine also regulates AP-1 activity, through which it not only enhances SOD and antiapoptotic Bcl-2 expression to prevent tubular cells from IR-induced apoptosis, but also promotes IL-10 expression to limit inflammatory response. Together, our data support that the administration of aloperine prior to IR insults such as renal transplantation could be a viable approach to prevent IR-induced injuries in clinical settings.

ACKNOWLEDGMENTS

This work was supported by grants from the National Natural Science Foundation of China (81130014, 81471046 and 81530024), the European Foundation for the Study of Diabetes (EFSD)/Chinese Diabetes Society (CDC)/Lilly Program for Collaborative Diabetes Research between China and Europe, and Innovative Funding for Translational Research from Tongji Hospital.

DISCLOSURE

The authors declare that they have no competing interests as defined by *Molecular Medicine*, or other interests that might be perceived to influence the results and discussion reported in this paper.

REFERENCES

1. Glaser DS. (1996) Acute renal failure. *N. Engl. J. Med*. 335:1321; author reply 1321–2.
2. Mangano CM, *et al*. (1998) Renal dysfunction after myocardial revascularization: risk factors, adverse outcomes, and hospital resource utilization. The Multicenter Study of Perioperative Ischemia Research Group. *Ann. Intern. Med*. 128:194–203.
3. Aydin Z, van Zonneveld AJ, de Fijter JW, Rabelink TJ. (2007) New horizons in prevention and treatment of ischaemic injury to kidney transplants. *Nephrol. Dial. Transplant*. 22:342–6.
4. Drazen JM, Ingelfinger JR, Curfman GD. (2003) Expression of concern: Schiffl H, et Al. Daily hemodialysis and the outcome of acute renal failure. N. Engl. J. Med. 346:305–10. *N. Engl. J. Med*. 348:2137.
5. Kazmers A, Jacobs L, Perkins A. (1997) The impact of complications after vascular surgery in Veterans Affairs Medical Centers. *J. Surg. Res*. 67:62–6.
6. Chertow GM, *et al*. (2005) Acute kidney injury, mortality, length of stay, and costs in hospitalized patients. *J. Am. Soc. Nephrol*. 16:3365–70.
7. Thurman JM, *et al*. (2006) Altered renal tubular expression of the complement inhibitor Crry permits complement activation after ischemia/reperfusion. *J. Clin. Invest*. 116:357–68.
8. Li L, *et al*. (2007) NKT cell activation mediates neutrophil IFN-gamma production and renal ischemia-reperfusion injury. *J. Immunol*. 178:5899–911.
9. Kelly KJ, *et al*. (1996) Intercellular adhesion molecule-1-deficient mice are protected against ischemic renal injury. *J. Clin. Invest*. 97:1056–63.
10. Day YJ, *et al*. (2005) Renal ischemia-reperfusion injury and adenosine 2A receptor-mediated tissue protection: role of macrophages. *Am. J. Physiol. Renal Physiol*. 288:F722–31.
11. Day YJ, *et al*. (2006) Renal ischemia-reperfusion injury and adenosine 2A receptor-mediated tissue protection: the role of CD4+ T cells and IFN-gamma. *J. Immunol*. 176:3108–14.
12. El Sabbahy M, Vaidya VS. (2011) Ischemic kidney injury and mechanisms of tissue repair. *Wiley Interdiscip. Rev. Syst. Biol. Med*. 3:606–18.
13. Kusch A, *et al*. (2013) Novel signalling mechanisms and targets in renal ischaemia and reperfusion injury. *Acta Physiol. (Oxf)*. 208:25–40.
14. Fan LH, *et al*. (2012) Effect of ischemia preconditioning on renal ischemia/reperfusion injury in rats. *Int. Braz. J. Urol*. 38:842–54.
15. Amura CR, *et al*. (2012) Complement activation and toll-like receptor-2 signaling contribute to cytokine production after renal ischemia/reperfusion. *Mol. Immunol*. 52:249–57.
16. Lu CY, Hartono J, Senitko M, Chen J. (2007) The inflammatory response to ischemic acute kidney injury: a result of the 'right stuff' in the 'wrong place'? *Curr. Opin. Nephrol. Hypertens*. 16:83–9.
17. Thurman JM. (2007) Triggers of inflammation after renal ischemia/reperfusion. *Clin. Immunol*. 123:7–13.
18. Liang CJ, *et al*. (2014) Endothelial progenitor cells derived from Wharton's jelly of human umbilical cord attenuate ischemic acute kidney injury by increasing vascularization and decreasing apoptosis, inflammation, and fibrosis. *Cell Transplant*. 24:1363–77.
19. Du T, Zhu YJ. (2014) The regulation of inflammatory mediators in acute kidney injury via exogenous mesenchymal stem cells. *Mediators Inflamm*. 2014:261697.
20. Thadhani R, Pascual M, Bonventre JV. (1996) Acute renal failure. *N. Engl. J. Med*. 334:1448–60.
21. Zhang CL, *et al*. (2012) Protective effects of garlic oil on hepatocarcinoma induced by N-nitrosodiethylamine in rats. *Int. J. Biol. Sci*. 8:363–74.
22. Chatterjee PK, *et al*. (2000) Tempol, a membrane-permeable radical scavenger, reduces oxidant stress-mediated renal dysfunction and injury in the rat. *Kidney Int*. 58:658–73.
23. Bo CJ, *et al*. (2013) Effects of ischemic preconditioning in the late phase on homing of endothelial progenitor cells in renal ischemia/reperfusion injury. *Transplant Proc*. 45:511–6.
24. Li C, *et al*. (2011) Sophocarpine administration preserves myocardial function from ischemia-reperfusion in rats via NF-kappaB inactivation. *J. Ethnopharmacol*. 135:620–5.
25. Zhou Y, *et al*. (2010) Total alkaloids of Sophora alopecuroides increases the expression of CD4+ CD25+ Tregs and IL-10 in rats with experimental colitis. *Am. J. Chin. Med*. 38:265–77.
26. Lin Z, Huang CF, Liu XS, Jiang J. (2011) In vitro anti-tumour activities of quinolizidine alkaloids derived from Sophora flavescens Ait. *Basic Clin. Pharmacol. Toxicol*. 108:304–9.
27. Yuan XY, *et al*. (2010) Effects and mechanisms of aloperine on 2, 4-dinitrofluorobenzene-induced allergic contact dermatitis in BALB/c mice. *Eur. J. Pharmacol*. 629:147–52.
28. Zhou CC, *et al*. (1989) [Anti-inflammatory and anti-allergic action of aloperine]. [Article in Chinese]. *Zhongguo Yao Li Xue Bao*. 10:360–5.
29. Qavi HB, Wyde PR, Khan MA. (2002) In vitro Inhibition of HHV-6 replication by sophocarpines. *Phytother. Res*. 16:154–6.
30. Qiong-Xu Y, *et al*. (2014) Aloperine attenuated neuropathic pain induced by chronic constriction injury via anti-oxidation activity and suppression of the nuclear factor kappa B pathway. *Biochem. Biophys. Res. Commun*. 451:568–73.
31. Meldrum KK, *et al*. (2001) A novel model of ischemia in renal tubular cells which closely parallels in vivo injury. *J. Surg. Res*. 99:288–93.
32. Wang LT, *et al*. (2013) Protective role of AMP-activated protein kinase-evoked autophagy on an in vitro model of ischemia/reperfusion-induced renal tubular cell injury. *PLoS One*. 8:e79814.

33. Li J, *et al*. (2011) Neutralization of the extracellular HMGB1 released by ischaemic damaged renal cells protects against renal ischaemia-reperfusion injury. *Nephrol. Dial. Transplant*. 26:469–78.
34. Zhong J, *et al*. (2014) MBD2 regulates TH17 differentiation and experimental autoimmune encephalomyelitis by controlling the homeostasis of T-bet/Hlx axis. *J. Autoimmun*. 53:95–104.
35. Zou R, *et al*. (2014) Telmisartan protects 5/6 Nx rats against renal injury by enhancing nNOS-derived NO generation via regulation of PPAR-gamma signaling. *Am. J. Transl. Res*. 6:517–27.
36. Zheng X, *et al*. (2006) Preventing renal ischemia-reperfusion injury using small interfering RNA by targeting complement 3 gene. *Am. J. Transplant*. 6:2099–108.
37. Yang J, *et al*. (2013) TJ0711, a novel vasodilatory beta-blocker, protects SHR rats against hypertension induced renal injury. *Am. J. Transl. Res*. 5:279–90.
38. Zhang S, *et al*. (2012) Loss of dicer exacerbates cyclophosphamide-induced bladder overactivity by enhancing purinergic signaling. *Am. J. Pathol*. 181:937–46.
39. Pandey D, *et al*. (2011) SUMO1 negatively regulates reactive oxygen species production from NADPH oxidases. *Arterioscler. Thromb. Vasc. Biol*. 31:1634–42.
40. Yang P, *et al*. (2013) Loss of Jak2 impairs endothelial function by attenuating Raf-1/MEK1/Sp-1 signaling along with altered eNOS activities. *Am. J. Pathol*. 183:617–25.
41. Zhang S, *et al*. (2009) HMGB1, an innate alarmin, in the pathogenesis of type 1 diabetes. *Int. J. Clin. Exp. Pathol*. 3:24–38.
42. Sharfuddin AA, Molitoris BA. (2011) Pathophysiology of ischemic acute kidney injury. *Nat. Rev. Nephrol*. 7:189–200.
43. Devarajan P. (2006) Update on mechanisms of ischemic acute kidney injury. *J. Am. Soc. Nephrol*. 17:1503–20.
44. Kim J, *et al*. (2006) Orchiectomy attenuates post-ischemic oxidative stress and ischemia/reperfusion injury in mice. A role for manganese superoxide dismutase. J *Biol. Chem*. 281:20349–56.
45. Wang X, *et al*. (2009) c-Fos enhances the survival of thymocytes during positive selection by upregulating Bcl-2. *Cell Res*. 19:340–7.
46. Wang ZY, *et al*. (2005) Regulation of IL-10 gene expression in Th2 cells by Jun proteins. *J. Immunol*. 174:2098–105.
47. Yu JH, Kim KH, Kim H. (2008) SOCS 3 and PPAR-gamma ligands inhibit the expression of IL-6 and TGF-beta1 by regulating JAK2/STAT3 signaling in pancreas. *Int. J. Biochem. Cell Biol*. 40:677–88.
48. Schroder K, Tschopp J. (2010) The inflammasomes. *Cell*. 140:821–32.
49. Zhang J. (2007) Yin and yang interplay of IFN-gamma in inflammation and autoimmune disease. *J. Clin. Invest*. 117:871–3.
50. Iyer SS, Cheng G. (2012) Role of interleukin 10 transcriptional regulation in inflammation and autoimmune disease. *Crit. Rev. Immunol*. 32:23–63.
51. Kezic A, Becker JU, Thaiss F. (2013) The effect of mTOR-inhibition on NF-kappaB activity in kidney ischemia-reperfusion injury in mice. *Transplant Proc*. 45:1708–14.
52. Zhang J, *et al*. (2013) Administration of dexamethasone protects mice against ischemia/reperfusion induced renal injury by suppressing PI3K/AKT signaling. *Int. J. Clin. Exp. Pathol*. 6:2366–75.
53. Chen J, *et al*. (2013) Low molecular weight fucoidan against renal ischemia-reperfusion injury via inhibition of the MAPK signaling pathway. *PLoS One*. 8:e56224.
54. Hao W, *et al*. (2006) Induction of apoptosis by the Ste20-like kinase SLK, a germinal center kinase that activates apoptosis signal-regulating kinase and p38. *J. Biol. Chem*. 281:3075–84.
55. Anitha M, *et al*. (2006) GDNF rescues hyperglycemia-induced diabetic enteric neuropathy through activation of the PI3K/Akt pathway. *J. Clin. Invest*. 116:344–56.
56. Chen L, *et al*. (2013) SYK inhibition modulates distinct PI3K/AKT- dependent survival pathways and cholesterol biosynthesis in diffuse large B cell lymphomas. *Cancer Cell*. 23:826–38.
57. Le Belle JE, *et al*. (2011) Proliferative neural stem cells have high endogenous ROS levels that regulate self-renewal and neurogenesis in a PI3K/Akt-dependant manner. *Cell Stem Cell*. 8:59–71.
58. She QB, *et al*. (2005) The BAD protein integrates survival signaling by EGFR/MAPK and PI3K/Akt kinase pathways in PTEN-deficient tumor cells. *Cancer Cell*. 8:287–97.
59. Hemmings BA, Restuccia DF. (2012) PI3K-PKB/Akt pathway. *Cold Spring Harb. Perspect. Biol*. 4:a011189.
60. Hirsch E, *et al*. (2000) Central role for G protein-coupled phosphoinositide 3-kinase gamma in inflammation. *Science*. 287:1049–53.
61. Weichhart T, Saemann MD. (2008) The PI3K/Akt/mTOR pathway in innate immune cells: emerging therapeutic applications. *Ann Rheum Dis*. 67 Suppl 3:iii70–4.
62. Doukas J, *et al*. (2006) Phosphoinositide 3-kinase gamma/delta inhibition limits infarct size after myocardial ischemia/reperfusion injury. *Proc. Natl. Acad. Sci. U. S. A*. 103:19866–71.
63. Ravingerova T, *et al*. (2012) PPAR-alpha activation as a preconditioning-like intervention in rats in vivo confers myocardial protection against acute ischaemia-reperfusion injury: involvement of PI3K-Akt. *Can. J. Physiol. Pharmacol*. 90:1135–44.
64. Libermann TA, Baltimore D. (1990) Activation of interleukin-6 gene expression through the NF-kappa B transcription factor. *Mol. Cell. Biol*. 10:2327–34.
65. Liang HL, *et al*. (2009) Partial attenuation of cytotoxicity and apoptosis by SOD1 in ischemic renal epithelial cells. *Apoptosis*. 14:1176–89.
66. Zhang L, *et al*. (2014) Aloperine induces G2/M phase cell cycle arrest and apoptosis in HCT116 human colon cancer cells. *Int. J. Mol. Med*. 33:1613–20.
67. Rui T, Kvietys PR. (2005) NFkappaB and AP-1 differentially contribute to the induction of Mn-SOD and eNOS during the development of oxidant tolerance. *FASEB J*. 19:1908–10.
68. Gu J, *et al*. (2011) Dexmedetomidine provides renoprotection against ischemia-reperfusion injury in mice. *Crit. Care*. 15:R153.

Cite this article as: Hu S, *et al*. (2015) Aloperine protects mice against ischemia-reperfusion (IR)-induced renal injury by regulating PI3K/AKT/mTOR signaling and AP-1 activity. *Mol. Med*. 21:912–23.